Research Paper https://doi.org/10.7733/jnfcwt.2017.15.4.343

Scaling Up Fabrication of UO_2 Porous Pellet With a Simulated Spent Fuel Composition

모의 사용후핵연료 조성의 UO_2 다공성펠렛 제조 스케일 업

Sang-Chae Jeon*, Jae-Won Lee, Joo-Young Yoon, and Yung-Zun Cho
Korea Atomic Energy Research Institute, 111, 989beon-gil, Yuseong-gu, Daejeon, Republic of Korea

전상채*, 이재원, 윤주영, 조용준
한국원자력연구원, 대전광역시 유성구 대덕대로 989번길 111

(Received Feburary 6, 2017 / Revised August 7, 2017 / Approved December 18, 2017)

Processing and equipment were tailored for engineering scale fabrication of UO_2 porous pellets, a feed material for the electrolytic reduction process in the PRIDE (PyRoprocessing Integrated DEmonstration) facility at KAERI (Korea Atomic Energy Research Institute). The starting materials, UO_2 powder and pre-milled surrogate oxide powders, were proportioned to simulate the chemical composition of spent fuel (so-called Simfuel). The Simfuel powders were homogenized by mixing, compacted into a pellet shape, and finally heat treated using a tumbling mixer, rotary press, and sintering furnace. After sintering at 1450℃ for 24 h in 4% H_2-Ar, the average bulk density of the UO_2 Simfuel pellets was 6.89 $g \cdot cm^{-3}$, which meets the standard of the following electrolytic reduction process. In addition, the results of a microstructural analysis demonstrated that the sintered Simfuel UO_2 porous pellets accurately simulate the properties of spent fuel in terms of the formation of second phases. These results provide essential information for the massive fabrication of UO_2 porous pellets for engineering scale pyroprocessing research.

Keywords: Pyroprocessing, Engineering scale, Head-end process, Feed material, Porous pellet

---

*Corresponding Author.
Sang-Chae Jeon, Korea Atomic Energy Research Institute, E-mail: scjeon@kaeri.re.kr, Tel: +82-42-866-6097

ORCID

Sang-Chae Jeon	http://orcid.org/0000-0002-9283-2546	Jae-Won Lee	http://orcid.org/ 0000-0002-3293-4540
Joo-Young Yoon	http://orcid.org/ 0000-0003-1932-3742	Yung-Zun Cho	http://orcid.org/ 0000-0003-2532-9489

This is an Open-Access article distributed under the terms of the Creative Commons Attribution Non-Commercial License (http://creativecommons.org/licenses/by-nc/3.0) which permits unrestricted non-commercial use, distribution, and reproduction in any medium, provided the original work is properly cited

KAERI의 PRIDE 시설에서 공학규모의 전해환원용 원료물질인 UO_2 다공성펠렛 제조를 위해 공정과 장치를 최적화시킨 내용을 다루었다. UO_2 분말과 별도로 attrition 밀링된 대용산화물 분말을 출발분말로, 정밀 칭량을 통해 사용후핵연료 조성을 모사하였다(Simfuel). Simfuel 분말은 각각 tumbling mixer로 혼합하여 균질화 하고, rotary press로 성형하여 furnace를 이용해 소결하였다. 4% H_2-Ar 분위기에서 1450℃ 24시간 고온 열처리하여 제조된 소결펠렛은 6.89 g · cm^{-3}의 벌크밀도를 가지며 이는 후속 전해환원 공정의 요구에 부합한다. 소결된 다공성펠렛의 미세구조 관찰을 통해 다공성 기지상과 함께 산화/금속 석출물이 관찰되어 사용후핵연료의 상이 모사됨을 확인하였다. 본 결과는 향후 공학규모 이상의 파이로 연구를 위한 UO_2 다공성펠렛 제조에 중요한 기초자료로 활용 될 것이다.

중심단어: 파이로프로세싱, 공학규모, 전처리공정, 원료물질, 다공성펠렛

1. Introduction

Pyroprocessing, a nuclear reprocessing technology, has attracted the interest of researchers both in academia and industrial circles due to its advantages: enhancing resource-use efficiency while reducing the volume and toxicity of nuclear waste with less proliferation risk than the PUREX reprocessing technology. Pyroprocessing generally consists of several unit processes; head-end process, electrolytic reduction, electrorefining, electrowinning, and treatment of waste. During the first head-end process, the spent fuel is recovered from the cladding hull and converted into an oxide feed material for the following electrolytic reduction process. The feed material is then electrochemically reduced to metal form in a molten salt followed by other unit processes to recycle the useful resources in the spent fuel by utilizing them as fuels for sodium-cooled fast reactor [1-4].

For the eventual success in the realization of pyroprocessing, its unit processes must be confirmed strictly including in all aspects: technical stability, environmental sustainability, and economic efficiency in a wide range of scale (from a lab to an enlarged scale). There have been many attempts to study the unit or partially integrated processes of pyroprocessing on lab scales. Based on the lab scale experience, KAERI constructed an engineering scale demonstration facility (PRIDE) for engineering scale pyroprocessing. The pyroprocessing in PRIDE is similar with the general case from head-end to waste treatment. During the first head-end process, a feed material for the following electrolytic reduction process should be prepared. Fragments, granules, and porous pellets are among the available physical forms of the feed material [4-11]. Although each form has respective strengths and drawbacks depending on its physical properties, the porous pellet is considered a superior feed form due to its well-known advantages as described in [12]. In addition to the general advantages, to be a successful practical feed material in the PRIDE facility, the porous pellet should have not only proper bulk and tap density for mass production but also similar chemical characteristics with regard to spent fuel consisting of the UO_2 matrix dissolved in other oxides, oxide and metal precipitates. These physical and chemical properties were considered as the criteria for the suitability of the produced UO_2 Simfuel porous pellet as a feed material for the electrolytic reduction in the PRIDE. In the head-end process, the chemical state of the starting material can be varied by final pre-treatment of the starting material UO_2 after reduction and U_3O_8 after oxidation. It is therefore necessary to fabricate the porous pellet with both uranium oxides (UO_2 and U_3O_8) as starting material. Previously, we fabricated UO_2 porous pellets on an engineering scale with the U_3O_8 powder as a starting material for pelletizing in the PRIDE facility [11].

The present work deals with the engineering scale fab-

Table 1. Fabrication process of simfuel porous pellet and the chemical/physical variations of product

Process	Preparation of starting material			Mixing	Pelletizing	Sintering
Material	Surrogates/ raw powders	Surrogates/ mixed powders	Surrogates/ milled powders	UO_2 + Surrogates + EBS* /powder	UO_2 + Surrogates + EBS* /pellet	UO_2 + Surrogates /porous pellet
		UO_2/ raw powder				
Equipment	Balance	Tubular mixer	Attrition mill	Tumbling mixer	Rotary press	Double chamber furnace

* Ethylene bis Stearamide, $(CH_2NHC(O)C_{19}H_{35})_2$

Table 2. The particle size of surrogate oxide powders

Element	Measured (μm)		Specification (μm)
	Mean Diameter	Standard Deviation	Mean Diameter
Y_2O_3	12.26	9.871	< 10
La_2O_3	16.34	13.53	5~15
CeO_2	28.64	19.99	14
Pr_6O_{11}	14.7	9.553	NA
Nd_2O_3	5.674	3.467	< 45
Sm_2O_3	25.7	36.25	5~15
Eu_2O_3	6.607	5.608	5~15
Gd_2O_3	7.259	6.745	< 10
SrO	38.09	36.48	< 150
ZrO_2	8.629	8.416	15~25
MoO_3	42.43	33.44	4~8
RuO_2	5.389	4.392	NA
Rh_2O_3	202.3	153.7	NA
PdO	50.43	29.35	< 75
TeO_2	28	15.65	NA

rication of UO_2 porous pellets (30 kg-U/batch) with UO_2 powder as a starting material for the electrolytic reduction process in the PRIDE facility. This includes modifications of the processing and equipment during each unit process and reflection of these changes on the products. The produced porous pellet was characterized physically and chemically to evaluate the processing, equipment and also the product in terms of the suitability for the electrolytic reduction in a molten salt. This work is therefore carried out not only to supply the feed material in the PRIDE facility but also to provide collective information on tailoring the fabrication process and related equipment for the mass production of UO_2 porous pellets for pyroprocessing research on an engineering scale.

Table 3. Chemical composition of the starting material (simulated burn-up: 55,000 MWd/tU, enrichment: 4.5%, cooling period: 10 years)

Fission product group	Element	Surrogate oxide	Fraction (wt%, oxide basis)
Dissolved oxides	U	UO_2	95.3253
	Y	Y_2O_3	0.0815
	La	La_2O_3	0.2077
	Ce	CeO_2	0.4275
	Pr	Pr_6O_{11}	0.1956
	Nd	Nd_2O_3	0.6901
	Sm	Sm_2O_3	0.1386
	Eu	Eu_2O_3	0.0232
	Gd	Gd_2O_3	0.0275
Oxide precipitates	Sr	SrO	0.1260
	Zr	ZrO_2	0.7107
	Ba	BaO	0.3018
Oxide/Metallic precipitates	Mo	MoO_3	0.7357
Metallic precipitates	Ru	RuO_2	0.5886
	Rh	Rh_2O_3	0.0762
	Pd	PdO	0.2572
Oxide/Metallic precipitates	Te	TeO_2	0.0868
	Total		100

2. Experimental

The UO_2 Simfuel porous pellets were fabricated on an engineering scale via a process that is similar to conventional ceramic processing with some improvements [11]. Table 1 shows the overall fabrication flow including the material and equipment in each unit process for the porous pellet in the PRIDE facility. The fabrication process in this work consists of four sequential unit processes: preparation of starting materials, mixing, pelletizing, and sintering. DU UO_2 powder and surrogate oxide powders were prepared as starting materials. Table 2 shows the particle size of the surrogate oxide powders measured by laser diffraction method (Beckman LS-230, USA) including comparison with their specifications. Before mixing with the DU UO_2 powder, the surrogate oxide powders were precisely proportioned according to the results calculated by ORIGEN (Oak Ridge Isotope Generation and Depletion) code (v. ORIGEN-ARP 5.1.01). The purity of the surrogate powders were: 99.999% for Y_2O_3, 99.99% for La_2O_3, CeO_2, and TeO_2, 99.95% for MoO_3, 99.9% for Pr_6O_{11}, Nd_2O_3, Sm_2O_3, Eu_2O_3, Gd_2O_3, MoO_3, RuO_2, Rh_2O_3, and PdO, 99.8% for BaO, 99.5% for SrO, and 99% for ZrO_2. The proportioned surrogate powders were mixed in a Turbula mixer and attrition-milled for 4 h in a high purity ethanol medium with 5 mm ZrO_2 balls before being mixed with UO_2 powder. After drying with a hot plate and a drying oven for 24 h, the milled surrogate oxide powders were mixed with UO_2 powder in a tumbling mixer for 4 h with a rotation speed of 38 rpm and then mixed 30 min more with the addition of 0.4wt% of

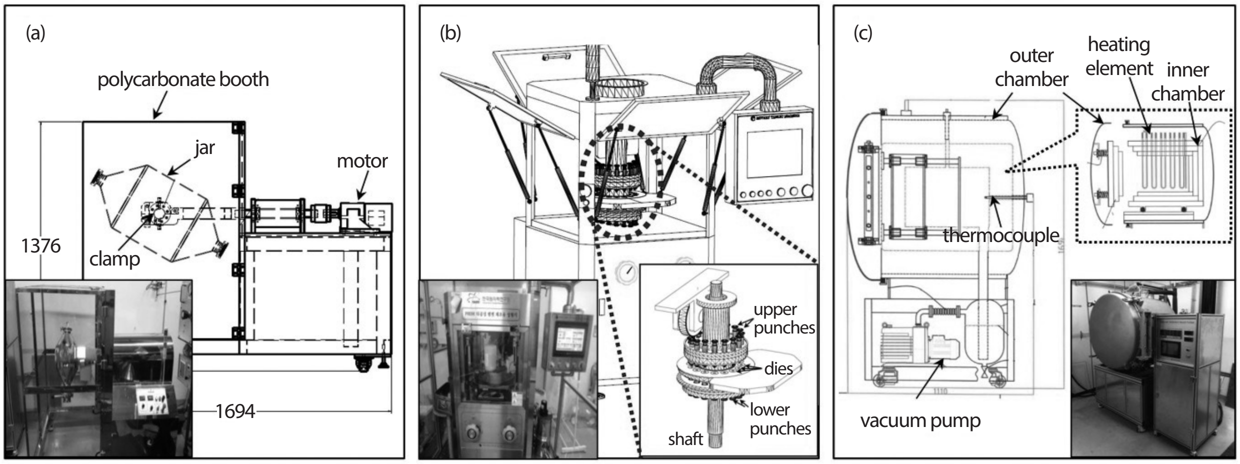

Fig. 1. Schematic drawings and photographs of (a) Tumbling mixer, (b) Rotary press, and (c) Double chamber furnace.

EBS (ethylene bis stearamide, $C_{38}H_{76}O_2N_2$, CAS no. 110-30-5) as a lubricant. The homogeneously mixed powders were pelletized using a rotary press. To improve the filling uniformity of the powder when it is put in a die hole, a mechanical feeder system was installed, as described in our previous report, for better flowability of the mixed powder [11]. The powder filled in the die hole was compacted by upper and lower punches at a range of 200-500 MPa pressure. Thirteen green pellets were produced by the 13 punch/die sets with rotation of the driving part using the rotary press. The green pellets were put into molybdenum crucibles that can hold ~13 kg of pellets and sintered in a double chamber furnace at 1450℃ for 24 h in a 4% H_2-Ar balanced atmosphere.

The microstructures of the sintered porous pellet were observed by SEM (Philips XL-30, Netherlands) and EDS (Energy Dispersive Spectroscope) attached on the SEM from the fracture surface of the pellet after vertical crushing. The crystal structure of the pellets was observed by XRD (Rigaku Mini-Flex, Japan) over the two theta range of 20~80° and at a scan speed of $6^{o}\cdot min^{-1}$ and a step size of 0.01° after crushing the sintered pellet in an agate mortar and pestle. The bulk density of the pellet was measured by the general water immersion method and was also calculated from the weight and dimensions of the pellet. The average value was determined by measuring 10 randomly sampled pellets.

3. Results and Discussion

The fabrication of the UO_2 porous pellet with a Simfuel composition in this study was carried out according to the fabrication process described in Table 1 with a composition of Table 3 that simulates the chemical composition of spent fuel. For the preparation of starting materials, DU UO_2 powder was prepared without any pre-treatment while the surrogate oxide powders were mixed and milled due to their large particle sizes as shown in Table 2. The large particles may result in drawbacks during the following pelletizing process. In the case of the DU UO_2 powder, its physical properties were analyzed: O/U ratio, surface area, and water content were measured as 2.196, 2.51 ($m^2\cdot g^{-1}$), and 3190 (ppm), respectively. This slightly larger O/U ratio than 2 of normal UO_2 indicates the surface of the UO_2 particles is slightly oxidized and includes UO_{2+x} and U_4O_{9-y} phases. The lower surface area and higher water content compared to the ADU UO_2 powder [13] would cause poor compactability and sinterability in the following unit processes.

Fig. 1 shows schematic drawings and photographs of

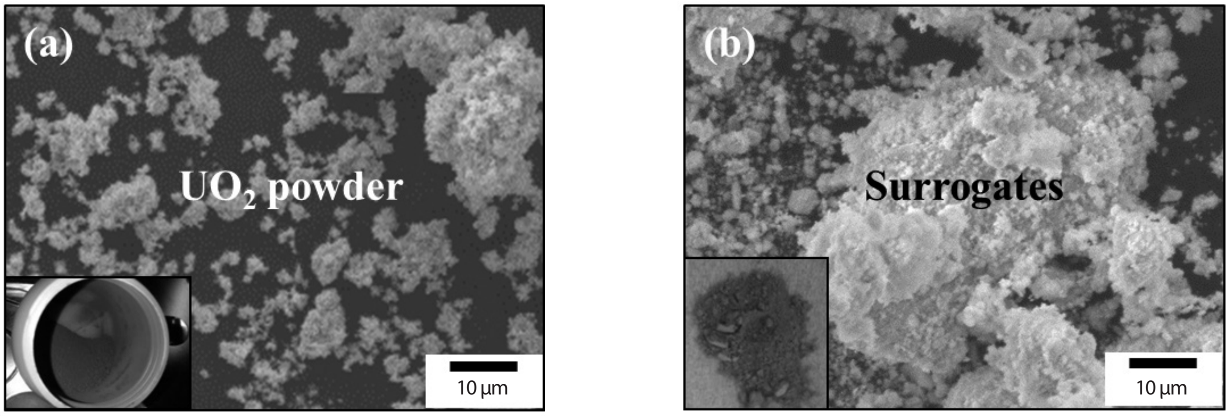

Fig. 2. SEM micrographs of (a) UO_2 and (b) Surrogate oxide powders.

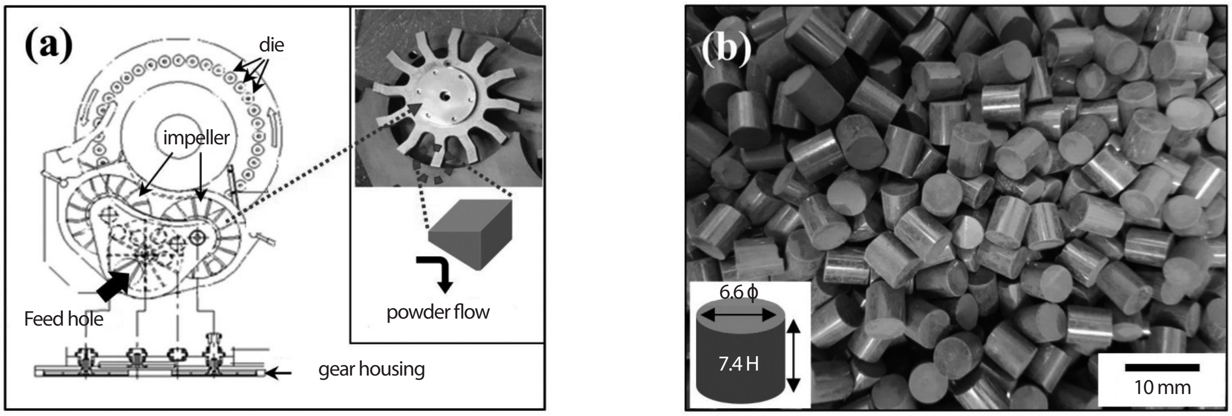

Fig. 3. (a) Schematic drawings and a photograph of the mechanical feeder attached to rotary press and (b) Produced UO_2 green pellets.

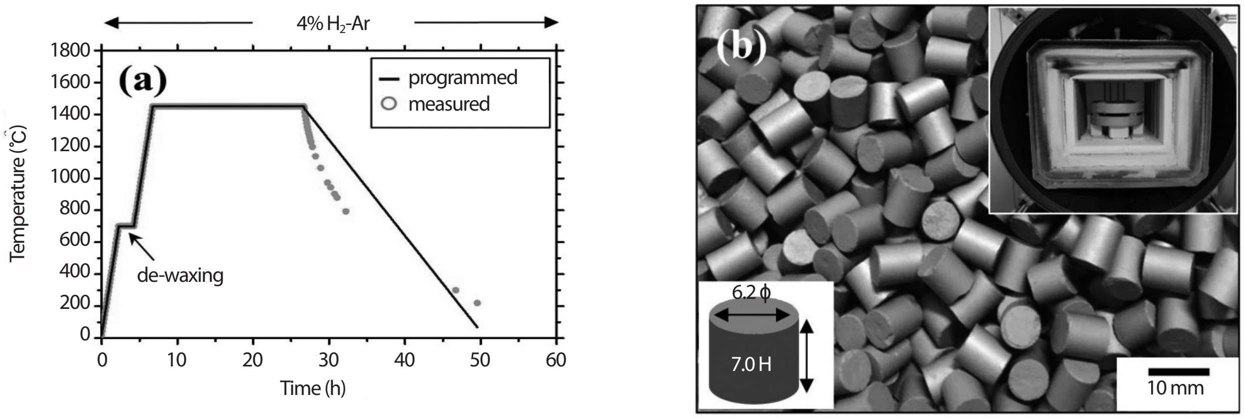

Fig. 4. (a) Thermal profile of sintering process and (b) Produced UO_2 sintered pellets with a simfuel composition.

the constructed equipment in the PRIDE facility. The UO_2 and surrogate powders were mixed using a tumbling mixer, shown in Fig. 1 (a), which is equipped with a driving motor, rotating shaft, and mixing jar. The mixed powder was compacted into a pellet shape by the rotary press shown in Fig. 1 (b). The concept of the equipment is similar to that of the commercial press machine used in pharmaceutical fields. The driving part contains 13 punch/die sets to uniaxially press the powder with the rotation shaft at a high production yield. The green pellets were then sintered in a furnace with a double chamber structure, as shown in Fig. 1 (c). The schematic drawings show both outer and inner views presenting the mechanical gate structure and refractories with heating element, respectively.

Fig. 2 shows SEM micrographs of UO_2 and attrition milled surrogates before mixing them in the tumbling mixer. It is noted that the particle size of the starting materials appears to be up to ~ 30 μm for the attrition milled surrogates and a few microns for UO_2. The particle size of the raw surrogate powders measured by the laser diffraction method ranged from a few microns to a few hundreds of microns. The particle size therefore should be reduced to raise the mechanical stability of the green pellet after compaction. As a result of attrition milling of the surrogates as pre-treatment before mixing with UO_2, finer size was measured: the largest particle was about ~ 30 μm, as shown in Fig. 2 (b). The surrogate powders were then placed in an inclined mixing jar and mixed with UO_2 powder by rotation of the shaft. The powders were homogenized by diffusional mixing with the motion of individual particles when the mixing jar rotates. The continuous rotation provides the inclined plane with fresh powder, leading to intermixing of the powder particles. The mixing process has two different objects: the first mixing is carried out to mix the UO_2 powder and surrogates whereas the second is to mix the homogenized UO_2 and surrogate powders with EBS, which acts as a lubricant. In this experiment, the amount of added EBS was slightly higher (0.4wt%) than the usual amount (~ 0.2wt%) to enhance the compactibility during the following pelletizing process.

Fig. 3 presents details of the modification of the mechanical feeder and the produced green pellets with application of the modified feeder. The mechanical feeder is attached at the driving part of the rotary press to improve the flowability of powder during the pelletizing process. This helps the powder supplied from the feeder move to the die holes by sweeping motion of the impeller wings. The cross sectional shape of the impeller wings in the mechanical feeder strongly affects the sweeping behavior and therefore the powder filling behavior. Three different impeller wing shapes, two rectangular shapes (with and without inclined plane) and a triangular shape, were compared and it was thereupon concluded that the rectangular shape with an inclined plane shown in Fig. 3 (a) provides superior powder filling behavior compared to the others. This is determined from the amount of the filled powder into the die holes and deviations. In the case of using the rectangular shape with an inclined plane, higher average weight of green pellets and smaller standard deviations were measured as 1.44 g and 0.07 g, respectively, from randomly sampled compacted green pellets. The compacted green pellets generally showed a smooth and glossy surface without any defects as shown in Fig. 3 (b). The green pellets were put into molybdenum crucibles to be sintered.

Fig. 4 presents a thermal profile of the sintering process and a photograph of sintered UO_2 porous pellets. High temperature heat treatment at 1450℃ was carried out after de-waxing at 700℃ for 24 hours in a reducing atmosphere using 4% H_2-Ar balanced gas. During sintering, the temperature and atmosphere were ensured by a double chamber structure: at inner chamber surrounded by refractories confined the heat while the outer chamber of stainless steel maintained the reducing atmosphere without leakage. As crucibles to stack a large amount of pellets, a molybdenum crucible of 3 mm thickness was designed with loosely assembled bottom and wall. There are also many holes at the bottom plane, allowing the green pellets to contact atmospheric gas by penetration of the gas through the holes, even when the crucibles are piled up vertically, as shown in

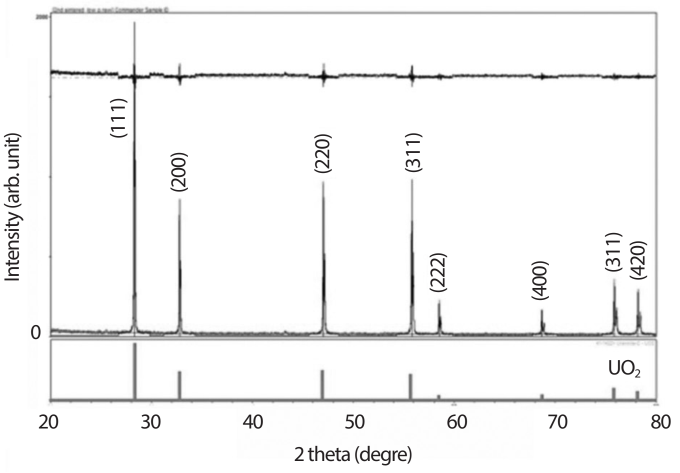

Fig. 5. XRD pattern of the UO_2 simfuel porous pellet after sintering.

Table 4. ICP-AES results of the sintered pellet

Element	Fraction (wt%, metal basis)			
	Pellet #1	Pellet #2	Pellet #3	Starting material
U	96.3413	96.5074	96.3192	95.7308
Y	0.0688	0.0689	0.0688	0.0741
La	0.1950	0.1838	0.1835	0.2043
Ce	0.4129	0.4136	0.4128	0.4014
Pr	0.1835	0.1723	0.1835	0.1867
Nd	0.6079	0.6089	0.6077	0.6823
Sm	0.1376	0.1379	0.1376	0.1379
Eu	0.0229	0.0230	0.0229	0.0231
Gd	0.0344	0.0230	0.0344	0.0275
Sr	0.1032	0.1149	0.1261	0.1229
Zr	0.5620	0.4366	0.4357	0.6069
Ba	0.2523	0.1723	0.3440	0.3117
Mo	0.4702	0.5055	0.5504	0.5656
Ru	0.3670	0.4481	0.4243	0.5157
Rh	0.0459	0.0574	0.0573	0.0712
Te	0.0115	0.0115	0.0115	0.0801
Total	100			

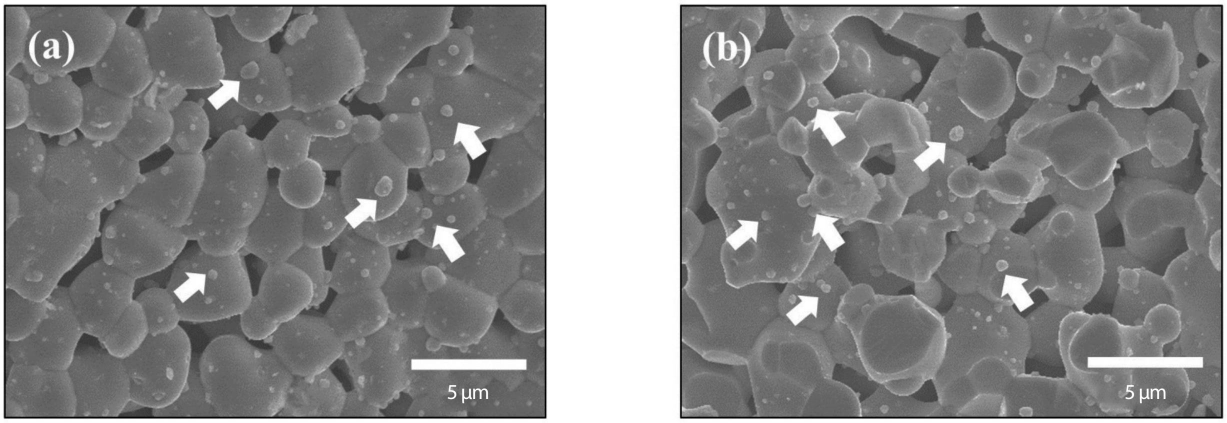

Fig. 6. SEM Micrographs Observed at the (a) Inside and (b) Surface of the Sintered Pellet.

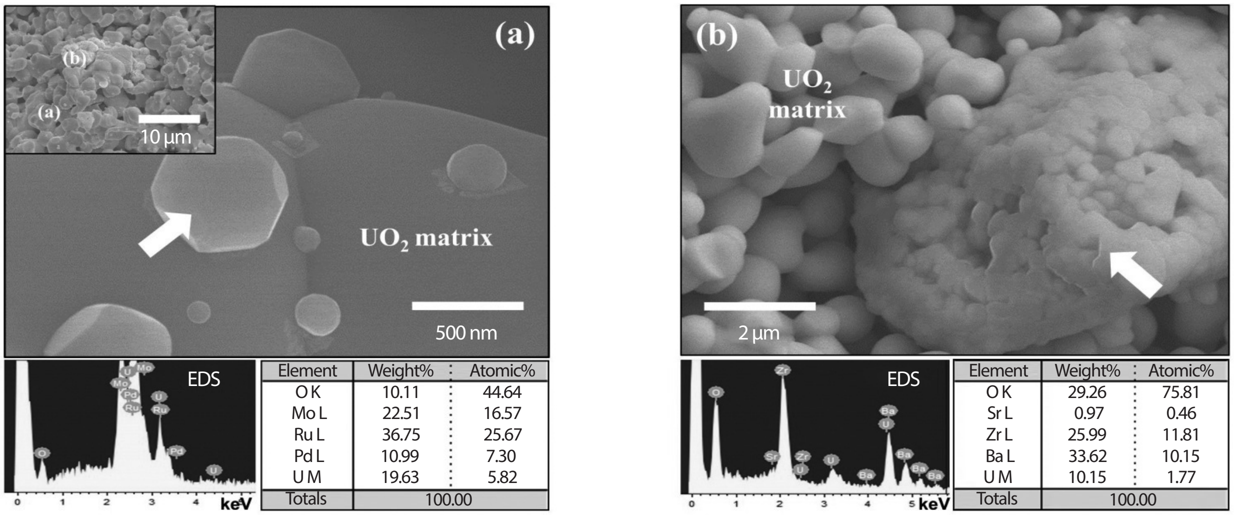

Element	Weight%	Atomic%
O K	10.11	44.64
Mo L	22.51	16.57
Ru L	36.75	25.67
Pd L	10.99	7.30
U M	19.63	5.82
Totals	100.00	

Element	Weight%	Atomic%
O K	29.26	75.81
Sr L	0.97	0.46
Zr L	25.99	11.81
Ba L	33.62	10.15
U M	10.15	1.77
Totals	100.00	

Fig. 7. SEM Micrographs on the Second Phases and EDS Results Thereof: Precipitates of (a) Metal and (b) Oxide Phase.

the inset in Fig. 4 (b). Temperature variations measured by a thermocouple at the inner chamber were consistent with the programmed behavior until the end of isothermal treatment. As a result of grain growth and densification during sintering, sintered UO_2 porous pellets with a Simfuel composition were obtained as shown in Fig. 4 (b).

The chemical and physical properties of the final product, i.e., a sintered UO_2 Simfuel porous pellet, were analyzed to evaluate its suitability for the following electrolytic reduction process as a feed material. The XRD pattern of the sintered pellet in Fig. 5 indicates a single UO_2 phase at the level of the XRD detection limit. It also suggests the reducing atmosphere was maintained without change during sintering. In addition, it is shown in Table 4 that the chemical composition values of three sintered pellets were similar and also similar to the starting material, indicating favorable chemical homogeneity. Although the boiling points of some surrogate oxides such as MoO_3, RuO_2, Rh_2O_3, and PdO are lower than the sintering temperature, their fraction appear to be maintained possibly due to increase of boiling points with their reduction to metallic phases before volatilization. In the case of TeO, however, its fraction was significantly decreased after sintering maybe due to preservative oxide phase, which has lower boiling point (~1245℃). The microstructures shown in Fig. 6 are observed at the (a) inside and (b) surface of the sintered pellet by SEM. Similar microstructures in terms of grain size and shape, apparent density, and presence of secondary phases (denoted as arrows) were obtained regardless of the position. These are typical grain and pore structure, grains connected with necks and interconnected pores among grains, suggesting the initial or intermediate stage of sintering. Compared to the initial particle size of UO_2 shown in Fig. 2 (a), the grain size slightly increased and the average bulk density also increased from the green pellet of 5.84 $g\cdot cm^{-3}$ (53.29% TD) to the sintered pellet of 6.89 $g\cdot cm^{-3}$ (62.94% TD). In this case, the tap density of the sintered pellets was 4.88 $g\cdot cm^{-3}$, which allows the pellets to be stacked in the cathode basket completely. The volume of the cathode basket has been determined based on the assumption that the tap density of feed materials would be of 4.5 $g\cdot cm^{-3}$. Therefore the produced Simfuel porous pellets could be loaded into the basket satisfying the intended processing scale of PRIDE facility. The secondary phases were characterized by an EDS attached to a SEM, as shown in Fig. 7. Fig. 7(a) shows the metal precipitates are located at the grain boundaries and junctions as protrusions on the UO_2 matrix grains. On the other hand, the oxide precipitate is shown in Fig. 7 (b) as bundles of small grains located between the matrix grains. Both are well distinguished by their morphology and are well-documented, typical characteristics of spent fuel, indicating the suitability of the UO_2 Simfuel porous pellet as a feed material for the electrolytic reduction experiment.

4. Conclusions

For the electrolytic reduction experiment in the PRIDE facility, the UO_2 Simfuel porous pellets have been fabricated successfully on an engineering scale with modifications of processing and equipment. Processing parameters and equipment were modified and optimized to secure production efficiency and processing stability with controlled product quality. As a final product, the UO_2 Simfuel porous pellet was characterized regarding the requirements of the electrolytic reduction process. Macroscopic properties such as size, density, and phase and microscopic grain/pore structure and distribution of the second phase meet the needs of engineering scale electrolytic reduction experiments in PRIDE.

Acknowledgement

This work was supported by the National Research Foundation of Korea (NRF) grant funded by the Korea government (MEST) (no. 2012M2A8A5025696).

REFERENCES

[1] K.C. Song, H. Lee, J.M. Hur, J.G. Kim, D.H. Ahn, and Y.Z. Cho, “Status of Pyroprocessing Technology Development in Korea”, Nucl. Eng. Technol., 42(2), 131-144 (2010).

[2] J.H. Yoo, C.S. Seo, E.H. Kim, and H.S. Lee, “A Conceptual Study of Pyroprocessing for Recovering Actinides from Spent Oxide Fuels”, Nucl. Eng. Technol., 40, 581-592 (2008).

[3] H. Lee, G.I. Park, K.H. Kang, J.M. Hur, J.G. Kim, D.H. Ahn, Y.Z. Cho, and E.H. Kim, “Pyroprocessing Technology Development at KAERI”, Nucl. Eng. Technol., 43(4), 317-328 (2011).

[4] E.Y. Choi, J.K. Kim, H.S. Im, I.K. Choi, S.H. Na, J.W. Lee, S.M. Jeong, and J.M. Hur, “Effect of the UO2 Form on the Electrochemical Reduction Rate in a LiCl–Li2O Molten Salt”, J. Nucl. Mater., 437, 178-187 (2013).

[5] S.D. Herrmann, S.X. Li, D.A. Sell, and B.R. Westphal, “Electrolytic Reduction of Spent Nuclear Oxide Fuel

– Effects of Fuel Form and Cathode Containment Materials on Bench-scale Operations", Proc. of Int. Conf. on Future Nucl. Systems, Global 2007, 758-762, Boise (2007).

[6] Y. Sakamura and T. Omori, "Electrolytic Reduction and Electrorefining of Uranium to Develop Pyrochemical Reprocessing of Oxide Fuels", Nucl. Techno., 171(3), 266–275 (2010)

[7] Y. Sakamura, "Effect of Alkali and Alkaline-Earth Chloride Addition on Electrolytic Reduction of UO2 in LiCl Salt Bath", J. Nucl. Mater. 412, 177-183 (2011).

[8] G. Uchiyama, M. Kitamura, K. Yamazaki, S. Torakai, S. Sugikawa, M. Maeda, and T. Tsujino, "Study on Voloxidation Process for Tritium Control in Reprocessing", Radioact. Waste Manage. Nucl. Fuel Cycle, 17, 63-79 (1992).

[9] J.J. Park, J.M. Shin, G.I. Park, J.W. Lee, and K.C. Song, "An Advanced Voloxidation Process at KAERI", Proc. of Int. Conf. on Future Nucl. Systems, Global 2009, 9161, Paris (2009).

[10] E.Y. Choi, J.W. Lee, J.J. Park, J.M. Hur, J.K. Kim, K.Y. Jung, and S.M. Jeong, "Electrochemical Reduction Behavior of a Highly Porous SIMFUEL Particle in a LiCl Molten Salt", Chem. Eng. J. 207-208, 514-520 (2012).

[11] S.C. Jeon, J.W. Lee, J.H. Lee, S.J. Kang, K.Y. Lee, Y.Z. Cho, D.H. Ahn, and K.C. Song, "Fabrication of UO2 Porous Pellets on a Scale of 30 kg-U/Batch at the PRIDE Facility", Adv. Mater. Sci. Eng., 2015, 1-8 (2015).

[12] S.C. Jeon, J.W. Lee, S.J. Kang, J.H. Lee, J.W. Lee, G.I. Park, and I.T. Kim, "Temperature Dependences of the Reduction Kinetics and Densification Behavior of U3O8 Pellets in Ar Atmosphere", Ceram. Int., 41, 657-662 (2015).

[13] Y.M. Pan, C.B. Ma, and N.N. Hsu, "The Conversion of UO2 via Ammonium Uranyl Carbonate: Study of Precipitation, Chemical Variation and Powder Properties," J. Nucl. Mater., 99, 135-147 (1981).